ELSEVIER

Contents lists available at ScienceDirect

Optical Materials

journal homepage: www.elsevier.com/locate/optmat



Research Article



Synthesis, properties and application of intense blue/green pigments based on Co/Cr doped Mg₂TiO₄ with excess MgO

Zhiwei Wang ^{a,1}, Qiuying Wang ^{a,1}, Yi Wang ^a, Theeranun Siritanon ^b, M.A. Subramanian ^c, Peng Jiang ^{a,*}

- a Department of Inorganic Nonmetallic Materials, School of Materials Science and Engineering, University of Science and Technology Beijing, Beijing, 100083, China
- b School of Chemistry, Institute of Science, Suranaree University of Technology, 111 University Avenue, Muang, Nakhon Ratchasima, 30000, Thailand
- ^c Department of Chemistry, Oregon State University, Corvallis, OR, 97330, USA

ARTICLE INFO

Keywords: Spinel structure Optical properties d-d transition Color PMMA composite

ABSTRACT

 $Mg_{2.2.x}Co_xTiO_4$ ($0 \le x \le 0.6$) and $Mg_{2.2.x}Cr_xTiO_4$ ($0 \le x \le 0.6$) solid solutions with spinel structure were successfully synthesized by solid-phase reaction. Excess MgO was added to achieve the single phase of the compounds. The transition metal ions Co/Cr tune the colors of Mg_2TiO_4 to intense blue and green, respectively. The root of the observed intense blue color of $Mg_{2.2.x}Co_xTiO_4$ is attributed to the 4A_2 (F) \rightarrow 4T_1 (P) transition of Co^{2+} in tetrahedral coordination. In Cr doped Mg_2TiO_4 , Cr exists in a mixed oxidation states of +3 and +6. The green color of the as-synthesized $Mg_{2.2.x}Cr_xTiO_4$ is attributed to 4A_2 (F) \rightarrow 4T_1 (F) at 410 nm–500 nm and 4A_2 (F) \rightarrow 4T_2 (F) at 610 nm transitions of Cr^{3+} . Besides, the Cr^{3+} - Ti^{4+} charge-transfer transition at 410 nm–500 nm is also the reason why it shows green. The as-synthesized pigments were dispersed into PMMA to prepare blue/green plastics.

1. Introduction

Due to high thermal and chemical stability, inorganic pigments are widely used in roof painting, ceramics, glass, plastics and other occasions [1]. Spinel is an ion-bound oxide, generally denoted as AB₂O₄. The arranged regularly tetrahedral and octahedral sites contribute to high chemical and thermal stability, as well as interesting optical properties. Therefore spinel oxides are widely used in catalyst, optical materials, transparent ceramics and other fields [2].

Previous researches were exerted on the preparation of blue and green inorganic pigments with Co and Cr spinel structure. The blue-green color solid solution of $\text{CoCr}_{2\text{-}x}\text{Al}_x\text{O}_4$ ($0 \le x \le 2$) spinel structure are synthesized by wet chemical method, and its potential for photocatalysis is also proved [3]. Furthermore, colorless ions such as Mg^{2+} and Zn^{2+} are introduced into Co site in Al-doped CoCrO_4 to reduce Co content by gel injection method [4,5]. Transition metals such as Ni, Cu and Zn are doped into Co site in $\text{Co}_{1\text{-}x}\text{M}_x\text{Cr}_2\text{O}_4$ (M = Ni, Cu and Zn) by sol-gel method to tune the color to blue-green and yellow-green, which shows potential as ceramic pigments [6].

The Co/Cr content of these pigments is lower than that of traditional

blue and green pigments such as CoAl₂O₄ and Cr₂O₃ [7]. At present, the preparation of inorganic pigments by adding a small amount of Co and Cr in spinel structure is more widely studied. Mg_{1-x}Zn_xAl_{1.8}Cr_{0.2}O₄ was synthesized by a gelpolymerization method. By introducing Zn, $Mg_{1-x}Zn_xAl_{1.8}Cr_{0.2}O_4$ changes the occupancy rate of Zn^{2+} , Mg^{2+} , and Al³⁺ in the tetrahedron and octahedron, thereby changing the crystal field environment and achieving tunable color [8]. Fe_{1-Ψ}Co_ΨCr₂O₄ (0 ≤ $\Psi \leq 1$) demonstrating red and blue color was synthesized by solution combustion synthesis method [9]. In addition, Huong doped Co(II) ions into the ZnAl₂O₄ spinel structure to obtain Zn_{1-x}Co_xAl₂O₄ blue pigments (x = 0.1, 0.3, 0.5, 0.7, 0.9). With the increase of Co(II) content, the intensity of blue gradually increased [10]. These methods are able to produce inorganic pigments with lower Co and Cr content. However, sol gel, water heat treatment and other methods are often used, which are complicated and requires accurate procedures. Therefore, it is eager to find new inorganic pigments that can be prepared with low content of Co and Cr and simple preparation process.

 Mg_2TiO_4 crystallizes in a typical inverse spinel structure (shown in Fig. 1), in which the oxygen ions are arranged in a cubic close pack. And half of Mg^{2+} occupies tetrahedra positions, and the other half of the

E-mail address: jiangp@ustb.edu.cn (P. Jiang).

^{*} Corresponding author.

¹ Zhiwei Wang and Qiuying Wang contributed equally to this work.

Z. Wang et al. Optical Materials 148 (2024) 114967

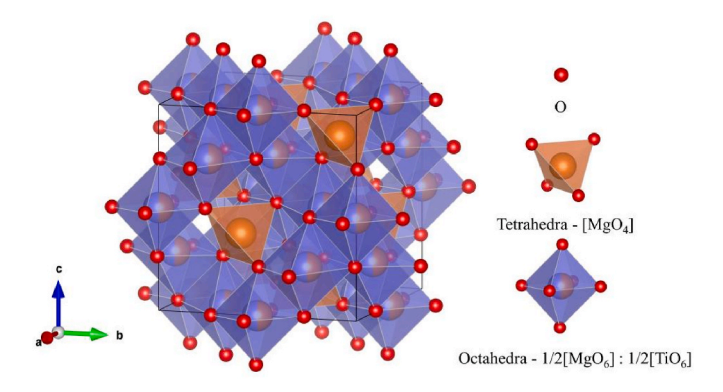


Fig. 1. Structure of Mg_2TiO_4 , red is oxygen atoms, orange is $[MgO_4]$ tetrahedra, purple is $[MgO_6]$ octahedral or $[TiO_6]$ octahedral.

Mg²⁺ and Ti⁴⁺ occupy octahedral positions. Mg²⁺ and Ti⁴⁺ randomly distribute at the octahedral positions in a 1:1 ratio. The spinel compound owns a relatively stable structure and can be used as high temperature refractory materials and electronic ceramic materials. It provides the structural basis for the isomorphic substitution of ions in lattices and therefore has a wide range of chromaticity fields as well as practical applications. Transition metal ion doping in spinel structure has been widely studied to prepare inorganic pigments with good color properties [11]. M. Llusar investigated nickel-doped spinel solid solutions prepared by solid-phase sintering and sol-gel methods as potential ceramic pigments or dyes [12].

Our research group has proved the contribution of spinel structure with Cr/Co doping in green/blue colored oxides. A new blue-green inorganic pigments was prepared by doping Cr/Co into the magneto plumbite BaMg₆Ti₆O₁₉ with spinel layers in the structure [13]. Wang et al. successfully synthesized a dark blue solid solution based on BaAl_{12-x}Co_xO₁₉ through a conventional solid-phase reaction. Its color developing mechanism is related to the d-d transition of Co in the spinel layer [14].

Therefore, in this work, novel blue/green pigments were synthesized by Co/Cr doped Mg_2TiO_4 through conventional solid state reaction. The as-prepared pigments were dispersed in PMMA to prepare color plastics. The mechanism of the observed intense colors are rationalized by XRD, XPS, UV–Vis spectra.

2. Experimental

2.1. Pigments preparation

 $Mg_{2.2\cdot x}Co_xTiO_4$ and $Mg_{2.2\cdot x}Cr_xTiO_4~(0\leq x\leq 0.6)$ compounds were prepared by conventional solid-state synthesis. The raw materials used are MgO (99.95 % purity, Aladdin, China), TiO_2 (99.99 % purity, Macklin, China), Co_3O_4 (99.99 % purity, Aladdin, China), and Cr_2O_3 (99.95 % purity, Aladdin, China). The mixed ingredients were first ground in an agate mortar. The mixed powder was then kept under a pressure of 10 MPa for 3 min to obtain a block sample. Subsequently, the samples were put in alumina crucibles and calcined at 1500 °C for 2 h.

2.2. PMMA composite preparation

BPO (benzoyl peroxide, 10.0 mg, AR purity, Aladdin, China) and MMA (methyl methacrylate, 10.0 mL, 99.0 % purity, Aladdin, China) were dissolved in glass flasks. Then, the as-synthesized pigments were added, and the glass flasks were placed in a water bath at 85 $^{\circ}$ C with magnetic stirring. When the mixture became glycerol-like, it was transferred to glass tubes. Then the glass tubes were placed in an oven. The mixture needed to cure at 50 $^{\circ}$ C for 24 h and react at 100 $^{\circ}$ C for 1 h. Finally, the rigid Poly (methyl methacrylate) (PMMA) stick was obtained by breaking the glass tube.

2.3. Characterization

The pigments were characterized by Rigaku Ultima IV X-ray diffractometer with Cu K α radiation ($\lambda=1.5406$ Å) to obtain X-ray diffractometion (XRD) patterns. The collection range is $10^{\circ}-90^{\circ}$. The scanning speed is $20^{\circ}/min$, and step size is 0.02° . The working voltage and current are 40 kV and 40 mA. The Binding energy of Co and Cr is obtained through X-ray photoelectron spectroscopy (XPS, ESCALAB 250XI).

 L^* a^* b^* color coordinates of samples were measured by a spectrophotometer (X-Rite Ci7600). In the three-dimensional model of CIE L^* a^* b^* , the L^* value indicates brightness. The a^* value from negative to positive represents a gradual transition from green to red. And the b^* value from negative to positive represents a gradual transition from blue to red. The UV–Vis–NIR absorbance spectra were obtained from a UV–Vis–NIR spectrometer (Hitachi UH4150). The wavelength range is between 200 and 2000 nm and barium sulfate (BaSO₄) was used for baseline correction.

The synthesized pigments were dispersed in prepared acetic acid (pH = 3) and ammonia (pH = 12) at room temperature and left to stand

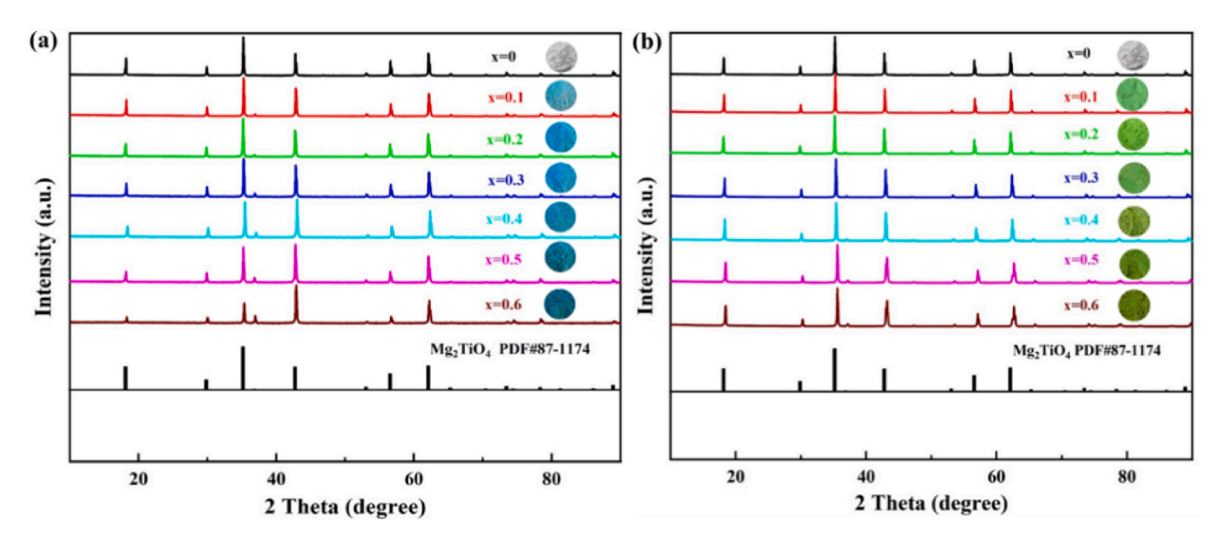


Fig. 2. XRD patterns of (a) $Mg_{2,2,x}Co_xTiO_4$ (0 $\leq x \leq 0.6$), (b) $Mg_{2,2,x}Cr_xTiO_4$ (0 $\leq x \leq 0.6$).

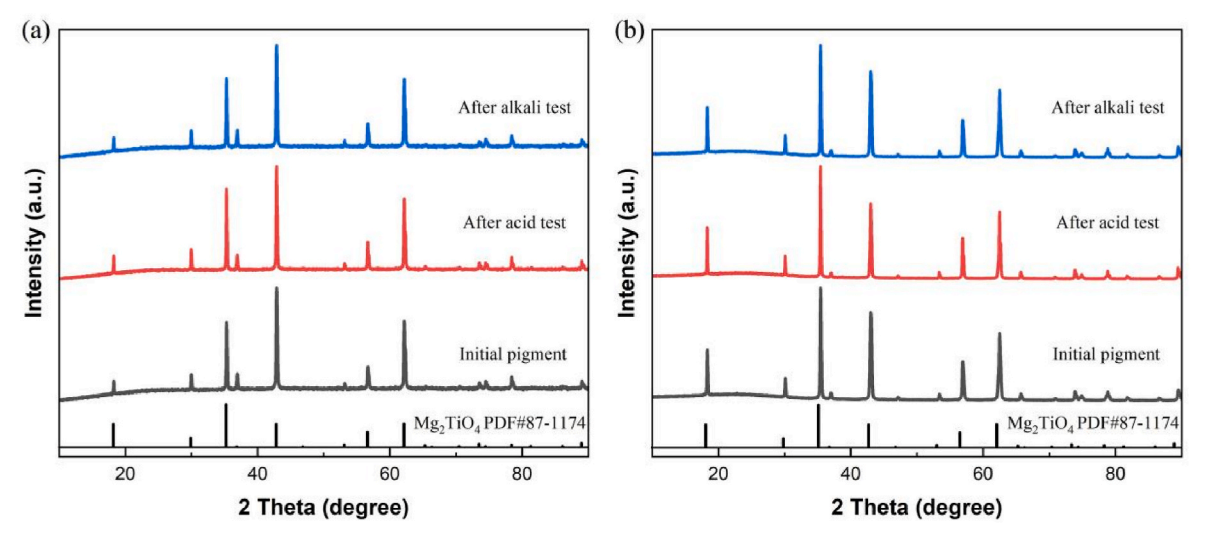
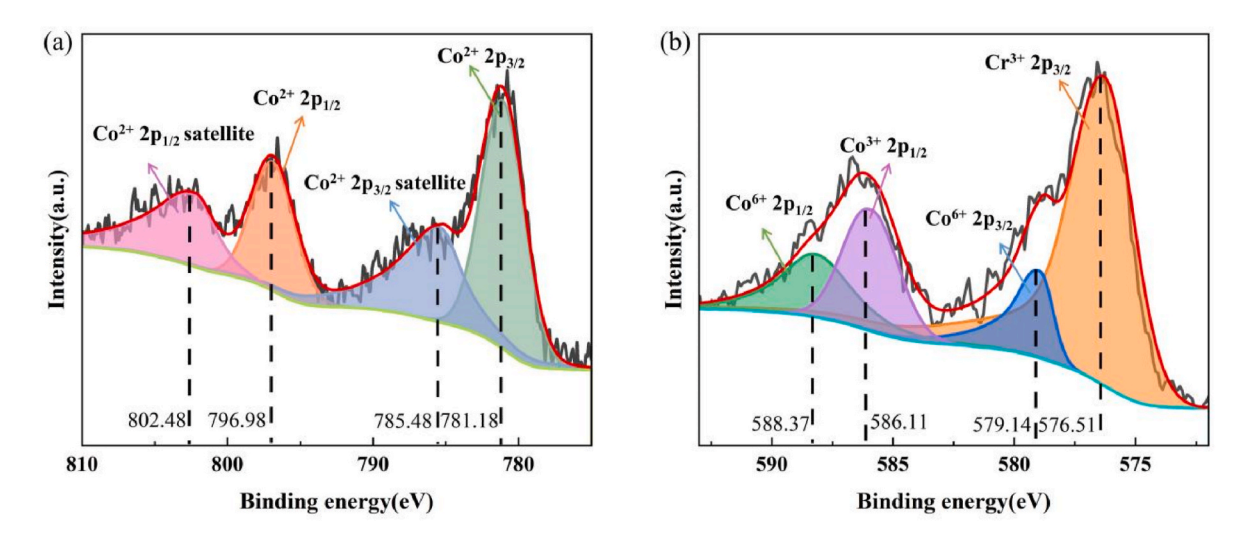


Fig. 3. XRD patterns of testing for leaching to acids and alkalis (a) Mg_{1.7}Co_{0.5}TiO₄, (b) Mg_{1.7}Cr_{0.5}TiO₄.



 $\textbf{Fig. 4.} \ \ \text{X-ray photoelectron spectra of (a) Co in } \ \ \text{Mg}_{1.8}\text{Co}_{0.4}\text{TiO}_{4}\text{, (b) Cr in } \ \text{Mg}_{1.8}\text{Cr}_{0.4}\text{TiO}_{4}\text{.}$

for 6 h. The samples were then washed with deionized water until the solution pH = 7. Finally, the samples were dried at 60 $^{\circ}\text{C}.$

3. Results and discussion

3.1. XRD analysis

The samples were first synthesized according to the stoichiometric ratio of Mg_2TiO_4 at $1500~^{\circ}C$ for 2 h. $MgTiO_3$ impurity was observed in the XRD of the as-synthesized samples. Excess MgO was then added to the formula to eliminate the impurity. When the formula reached to $Mg_{2.2}TiO_4$, single spinel structure pattern was achieved. Therefore, Co/Cr were designed to dope into the Mg site in $Mg_{2.2}TiO_4$. As shown in Fig. 2, the main peaks of all the samples are aligned with the hexagonal Mg_2TiO_4 with the space group of $Fd\overline{3}m$ (PDF#87-1174). The peaks correlated to impurities are not observed, proving that the synthesized samples are all pure phase. For Co/Cr doped $Mg_{2.2}TiO_4$, the maximum doping range is ($0 \le x \le 0.6$). As the doping amount of Co and Cr increases, new impurity peaks will appear, so the maximum doping amount is limited to 0.6. With the increase of doping amount, the color is gradually darkened.

To prove the acid-alkali resistance of the as-synthesized pigments, the pigments were soaked in acetic acid (pH=3) and ammonia (pH=

12) at room temperature for 6 h and the XRD patterns of samples before and after acid-alkali test are listed below. As shown in Fig. 3, the peak intensity and peak position did not change, indicating that the pigment has promising chemical stability.

3.2. XPS analysis

In order to analyze the valence state of doped ions in spinel structure, X-ray photoelectron spectroscopy was performed on Mg_{1.8}Co_{0.4}TiO₄ and Mg_{1.8}Cr_{0.4}TiO₄, and the Co and Cr 2p scans are shown in Fig. 4. In Mg_{1.8}Co_{0.4}TiO₄ in Fig. 4(a), after fitting, the Co 2p survey can be divided into four peaks. The binding energy peaks from high to low correspond to Co 2p 3/2 (781.18 eV), Co 2p 3/2 (785.48 eV) satellite, Co 2p 1/2 (796.48 eV), and Co 2p 1/2 satellite (802.48 eV), respectively. In Co₂Al₂O₄ prepared by sol-gel and solid-phase methods, the binding energies of Co 2p 3/2 are 781.7 eV and 781.4 eV, while the binding energies of 2p 1/2 are 797.36 eV and 797.18 eV [15,16]. In Mg_xCo_{1-x}. Al₂O₄ cobalt blue composite pigments, the binding energy of Co 2p 3/2 is observed as 781.26 eV [17]. Above reported results are similar to the observed value, so it is concluded that the valence state of Co ion in the synthesized products is +2.

In Mg_{1.8}Cr_{0.4}TiO₄ (Fig. 4(b)), two peaks corresponding to Cr 2p 3/2 and Cr 2p 1/2 are observed and each group of peaks splits into two

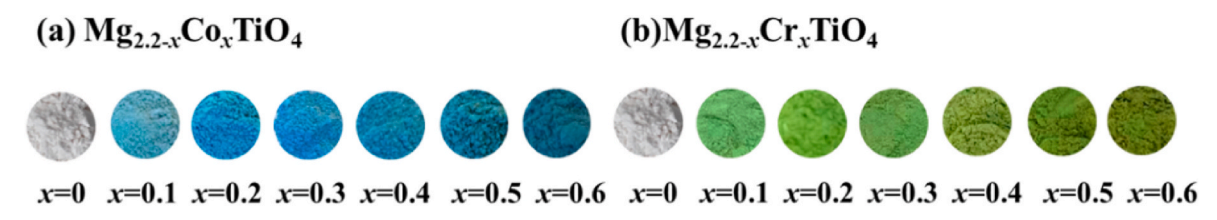


Fig. 5. The photographs of (a) $Mg_{2,2-x}Co_xTiO_4$ ($0 \le x \le 0.6$), (b) $Mg_{2,2-x}Cr_xTiO_4$ ($0 \le x \le 0.6$).

Table 1 The CIE L^* a^* b^* color coordinates of the powder pigments.

sample	L^*	a*	b*
Mg _{2.2} TiO ₄	91.92	-0.14	0.09
$Mg_2Co_{0.2}TiO_4$	50.87	-16.15	0.14
$Mg_2Co_{0.4}TiO_4$	60.47	-19.65	-2.05
$Mg_2Co_{0.6}TiO_4$	57.26	-14.57	-6.62
$Mg_2Cr_{0.2}TiO_4$	61.69	-5.42	17.03
$Mg_2Cr_{0.4}TiO_4$	64.37	-8.59	19.27
$Mg_2Cr_{0.6}TiO_4$	58.56	-10.2	17.7

values. Due to the higher sensitivity of electrons in the outer shell, the Cr 2p 3/2 peak is used to analyze the oxidation state of Cr. The binding energy of Cr 2p 3/2 at 576.51 eV is close to the Cr_2O_3 (576.6 eV) or $CrPO_4$ (578.3 eV) [18]. Thus, the occurrence of Cr^{3+} in $Mg_2Cr_{0.2}TiO_4$ could be confirmed. The binding energy at 579.14 eV is close to that of $Ca_3Co_{4-x}Cr_xO_9$ (579.7 eV) or K_2CrO_4 (579.1 eV) [18,19], indicating the presence of Cr^{6+} in the $Cr-Mg_2TiO_4$. Therefore, the presence of both Cr^{3+} and Cr^{6+} can be determined in $Mg_{1.8}Cr_{0.4}TiO_4$. Similar coexistence of Cr^{3+} and Cr^{6+} is also previously reported in $Mg(Al, Cr)_2O_4$ with spinel structure [20]. The portion of Cr ions in different oxidation state is related to the peak area in the X-ray photoelectron spectra. Therefore, it's obvious to find that the amount of Cr^{3+} is greater than Cr^{6+} .

3.3. Optical properties

The photographs of the $Mg_{2,2-x}Co_xTiO_4$ and $Mg_{2,2-x}Cr_xTiO_4$ ($0 \le x \le 0.6$) are shown in Fig. 5. The undoped $Mg_{2,2}TiO_4$ sample appears pure white. With elevated amount of Co doping, the color of the $Mg_{2,2-x}Co_xTiO_4$ pigments (Fig. 5 (a)) gradually changes from light blue (x = 0.5) gradually changes from light blue (x = 0.5).

0.1) to dark blue (x=0.6). The color of the $Mg_{2.2-x}Cr_xTiO_4$ column (Fig. 5 (b)) was adjusted from light green (x=0.1) to green (x=0.6) with increasing chromium content.

Table .1 provides a graphical representation of Co/Cr substitution for $Mg_{2.2}TiO_4$ oxides in the L^* a^* b^* value. The hues of a^* and b^* gradually deepen as they get farther away from the midpoint. With the increase of Cr concentration, the a^* value of $Mg_{2.2}$, Cr_xTiO_4 decreases, leading to a deep green color of the sample. The b^* value of $Mg_{2.2}$, Co_xTiO_4 is descending when the Co concentration is enhanced. These results are in accordance with the apparent color.

The UV–Vis–NIR spectra are analyzed to demonstrate the ligand field of Co and Cr ions. Existed in $3d^7$ configuration, Co^{2+} undergoes three spin-allowed transitions in both tetrahedral or octahedral ligand field. As $Mg_{2,2,x}Co_xTiO_4$ can provide tetrahedral and octahedral ligand fields for Co^{2+} , the determination of its ligand field is based on the characteristic transition. When Co^{2+} occupies the octahedral position, the 4T_1 (F) $\rightarrow ^4T_2$ (F), 4T_1 (F) $\rightarrow ^4A_2$ (F) and 4T_1 (F) $\rightarrow ^4T_1$ (P) transitions occur [21]. Additionally, the 4T_1 (F) $\rightarrow ^4A_2$ (P) transition can generate a characteristic peak that appears near 750 nm. This above listed peaks are observed in Co^{2+} in octahedral coordination in $CoTiO_3$ [22]. However, the absorption at 750 nm is not observed in the as-synthesized sample. Therefore, possibility of Co^{2+} in the octahedral site could be ruled out.

The Tanabe-Sugano (T-S) diagram of Co^{2+} (d^7 electron configuration) in tetrahedral coordination is shown in Fig. 6 (a). Under the action of tetrahedral coordination field, the d orbital splits into t_{2g} and e_g energy levels. During the d-d transition of Co^{2+} ion, the d orbital electrons transition from e_g to t_{2g} . The three spins that allow the Co^{2+} d-d transition are indexed to the d^7 electron configuration in the tetrahedral coordination (Fig. 6 (b)). The three spin allowed transitions are ${}^4\text{A}_2$ (F) \rightarrow ${}^4\text{T}_2$ (F), ${}^4\text{A}_2$ (F) \rightarrow ${}^4\text{T}_1$ (F), and ${}^4\text{A}_2$ (F) \rightarrow ${}^4\text{T}_1$ (P). Generally, similar

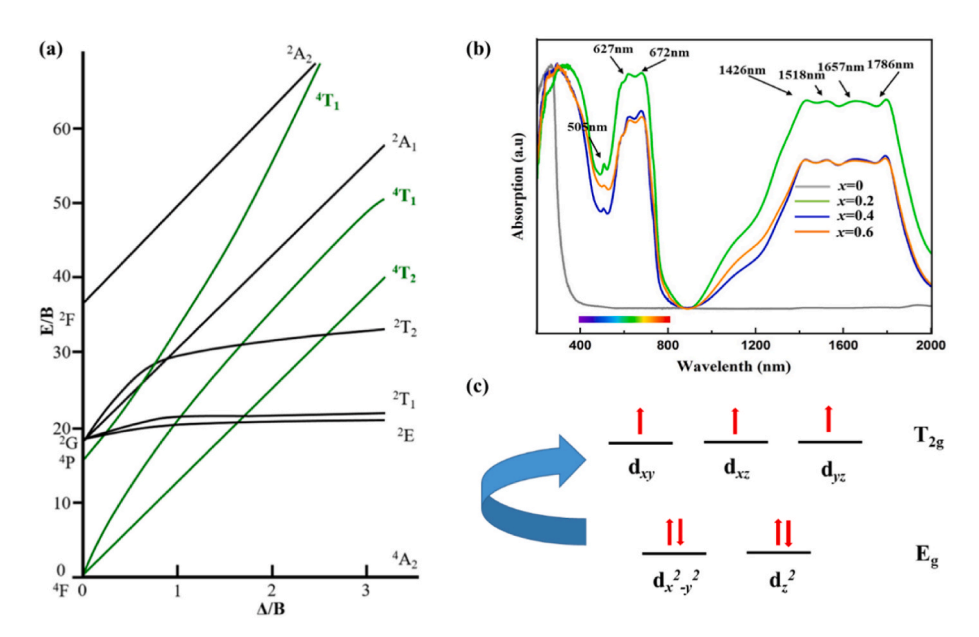


Fig. 6. (a) Tanabe-Sugano (T-S) diagram for Co^{2+} (d^7 electronic configuration) in tetrahedral coordination, (b) UV–Vis–NIR absorbance spectra of $Mg_{2.2-x}Co_xTiO_4$ (0 $\leq x \leq 0.6$), (c) d-d transition of Co^{2+} ion in tetrahedral structure.

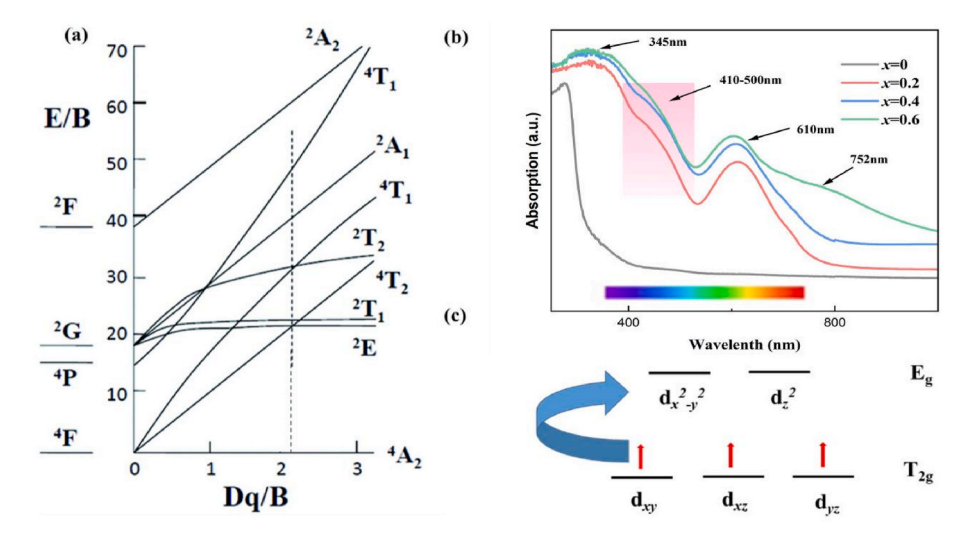


Fig. 7. (a) Tanabe-Sugano (T-S) diagram for Cr^{3+} (d^3 electronic configuration) in octahedral coordination, (b) UV–Vis–NIR absorbance spectra of $Mg_{2.2-x}Cr_xTiO_4$ (0 $\leq x \leq 0.6$), (c) d-d transition of Cr^{3+} ion in octahedral structure.

characteristic peaks are produced from ions in similar crystal field environments. However, because their crystal field environments are different, the position and intensity of their characteristic peaks will shift accordingly. The 4A_2 (F) $\rightarrow {}^4T_1$ (F) can produce a broad band at 1300-1700 nm region [23-25]. So the broad band at 1400-1800 nm in Fig. 6(b) is attributed to d-d transition ${}^{4}A_{2}(F) \rightarrow {}^{4}T_{1}(F)$. The transition of ${}^{4}A_{2}$ (F) (ground state) $\rightarrow {}^{4}T_{1}$ (P) has been found to split into a triplet signal in the visible wavelength region due to the Jahn-Teller distortion of the tetrahedral structure or the interaction between the L and S quantum numbers [26–28]. The 4A_2 (F) (ground state) \rightarrow 4T_1 (P) transition split into a triplet signal at 505 nm, 627 nm and 672 nm in $Mg_{2.2-x}Co_xTiO_4$. The 4A_2 (F) \rightarrow 4T_2 (F) tends to appear at 2500 nm [29]. So the transition isn't found in Fig. 6(b). The three bands in visible wavelength region and the broad band in infrared wavelength region are all attributed to the Co²⁺ in the tetrahedral position, so it is confirmed that Co²⁺ is in the tetrahedral ligand field.In Mg_{2,2-x}Cr_xTiO₄, Cr majorly exists in Cr3+ while a small amount of Cr resides in the form of Cr6+. However, the Cr⁶⁺ doesn't exhibit d-d transition because of $3d^0$ -configuration. The UV-Vis-NIR spectrum of the sample (Fig. 7 (b)) is similar to the absorption spectrum of Cr^{3+} in octahedral coordination [30]. The Tanabe-Sugano (T-S) diagram of Cr^{3+} (3 d^3 electron configuration) in octahedral coordination is shown in Fig. 7 (a). Under the action of octahedral coordination field, the d orbital splits into a higher e_g and lower t_{2g} level. The electron of Cr^{3+} ion in t_{2g} will absorb energy and jump up to e_g in a d-d transition. In the UV–Vis–NIR spectrum of the sample (Fig. 7 (b)), some absorption peaks can be observed. The ⁴A₂ (F) \rightarrow ⁴T₁ (F) transition is allowed to occur between 391 nm and 461 nm [30]. There is a broad absorption peak at 410 nm-500 nm. In addition to 4 A₂ (F) \rightarrow 4 T₁ (F) transition, the Cr³⁺-Ti⁴⁺ charge-transfer transition is also allowed to occur at 450 nm [31]. So, the broad absorption peak is caused by these two transitions. The ${}^4A_2(F) \rightarrow {}^4T_2(F)$, ${}^4A_2(F) \rightarrow {}^2T_1(G)$ and ${}^{4}A_{2}$ (F) \rightarrow ${}^{2}E$ (G) transitions also occur in the visible range. The former one normally ranges between 503 nm and 614 nm, and the latter two between 657 nm and 730 nm [30]. The ${}^{4}A_{2}(F) \rightarrow {}^{2}T_{1}(G)$ and ${}^{4}A_{2}(F)$ \rightarrow ²E (G) bands are often overlapped. So the bands at 610 nm and 752 nm are assigned to the ${}^4A_2(F) \rightarrow {}^4T_2(F)$, ${}^4A_2(F) \rightarrow {}^2T_1(G)$ and ${}^4A_2(F) \rightarrow$ 2 E (G) transitions. The absorption peak at 345 nm is due to 4 A₂ (F) \rightarrow 4 T₂ (P) transitions [32]. So, the Cr³⁺ is in the tetrahedral ligand field.

3.4. Colored PMMA composite

The 2 wt% of $Mg_{2.2.x}M_xTiO_4$ (M = Co or Cr, x = 0, 0.2, 0.4 and 0.6) pigments were dispersed in PMMA to produce color composite plastics. The color of the plastics and the colorimetric coordinates are shown in

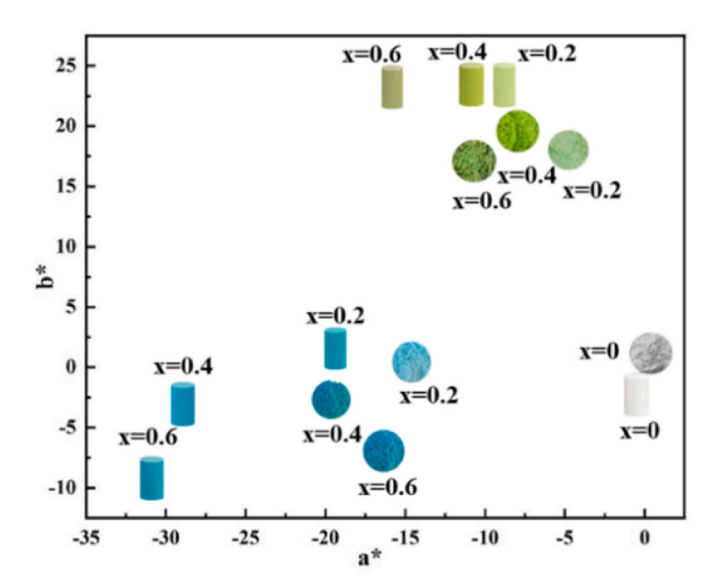


Fig. 8. PMMA composite color coordinates with objective colors in a^*b^* space.

Fig. 8. The colors of the plastics vary with the Co/Cr doping amount. With the increase of Cr doping amount, the samples show decrease in a^* value and increase in green color intensity. With increase in Co doping, it shows decrease in b^* value and corresponding increase in blue color intensity. For comparison in Fig. 8, the measured L^* a^* b^* values of PMMA are quite close to the pigment powder. The shift of L^* a^* b^* values is rooted in the encapsulation of the pigment particles in the PMMA matrix, which affects the absorption and reflection of light [33]. In addition, The apparent color of the PMMA is uniform (Fig. 9), so the pigments have good coloring properties for PMMA.

4. Summary and conclusions

In this work, single phase $Mg_{2.2-x}Co_xTiO_4$ and $Mg_{2.2-x}Cr_xTiO_4$ blue/green colored oxides with spinel structure were successfully prepared by solid-state reaction. Excess MgO is added to ensure the single phase of all the samples. The XPS results shows that Co states at the oxidation state of +2, while Cr resides in both +3 and +6 states. From the UV–Vis–NIR spectrum, the absorption peak at 505-700 nm from 4A_2 (F) \rightarrow 4T_1 (P) transition of Co^{2+} is the origin of the blue color. The absorption peak due

Fig. 9. Colors of pure PMMA and PMMA composite with 2 wt% Co/Cr doped Mg2.2TiO4 pigments.

to the 4A_2 (F) \rightarrow 4T_2 (F) transition of Cr^{3+} at 600 nm in the visible light range is the root of its green color. Subsequently, only 2 wt% pigments can make PMMA exhibit good color performance, indicating that the pigments has good coloring ability and good adaptability to plastics.

CRediT authorship contribution statement

Zhiwei Wang: Conceptualization, Investigation, Writing – original draft, Writing – review & editing. Qiuying Wang: Investigation, Methodology, Writing – original draft. Yi Wang: Investigation, Writing – original draft. Theeranun Siritanon: Supervision. M.A. Subramanian: Supervision, Writing – original draft. Peng Jiang: Resources, Supervision, Writing – original draft.

Declaration of competing interest

The authors declare that they have no known competing financial interests or personal relationships that could have appeared to influence the work reported in this paper.

Data availability

Data will be made available on request.

Acknowledgments

This work was sponsored by Beijing Nova Program under the grant number of 20230484282, the Fundamental Research Funds for the Central Universities under the grant number of FRF-IDRY-22-011, and Youth Teacher International Exchange & Growth Program under the grant No. QNXM20220018. The work done at Oregon State University is supported by US National Science Foundation Grant No. DMR-2025615.

References

- [1] S. Jose, D. Joshy, S.B. Narendranath, P.J.S.E.M. Periyat, S. Cells, Recent advances in infrared reflective inorganic pigments 194 (2019) 7–27.
- [2] Y. El Jabbar, H. Lakhlifi, R. El Ouatib, L. Er-Rakho, S. Guillemet-Fritsch, B.J.S.S. C. Durand, Preparation and characterisation of green nano-sized ceramic pigments with the spinel structure AB₂O₄ (A= Co, Ni and B= Cr, Al), 334 (2021) 114394.
- [3] Y. El Jabbar, H. Lakhlifi, R. El Ouatib, L. Er-Rakho, S. Guillemet-Fritsch, B.J.C. I. Durand, Green nanoceramic pigments based on cobalt chromite doped with Al: synthesis, characterisation and colour performance 47 (2021) 9373–9381.
- [4] X. Yin, J. Huang, Z. Pu, J. Li, H. Feng, X. Wang, Y. Wang, Effect of the calcination temperature on the cation distribution and optical properties of Mg_{0.5}Co_{0.5}CrAlO₄ spinel pigment, Ceram. Int. 47 (2021) 17167–17176.
- [5] H.R. Hedayati, A.A. Sabbagh Alvani, H. Sameie, R. Salimi, S. Moosakhani, F. Tabatabaee, A. Amiri Zarandi, Synthesis and characterization of Co_{1-x}Zn_xCr_{2-y}Al_yO₄ as a near-infrared reflective color tunable nano-pigment, Dyes Pigments 113 (2015) 588–595.
- [6] E. Grazenaite, J. Pinkas, A. Beganskiene, A. Kareiva, Sol-gel and sonochemically derived transition metal (Co, Ni, Cu, and Zn) chromites as pigments: a comparative study, Ceram. Int. 42 (2016) 9402–9412.
- [7] B. Bae, S. Tamura, N.J.C.I. Imanaka, Novel environmentally friendly inorganic yellow pigments based on gehlenite-type structure 42 (2016) 15104–15106.

- [8] T. Zhang, J. Huang, J. Yan, Z. Pu, X. Yin, Y. Wang, The structural evolution and optical properties of Mg_{1-x}Zn_xAl_{1.8}Cr_{0.2}O₄ pink ceramic pigments, Ceram. Int. 45 (2019) 16848–16854
- [9] S. Mestre, M.D. Palacios, P. Agut, Solution combustion synthesis of (Co,Fe)Cr₂O₄ pigments, J. Eur. Ceram. Soc. 32 (2012) 1995–1999.
- [10] D. Quy Huong, T. Duong, N.L.M. Linh, Rosin used as a potential organic precursor in synthesis of blue pigment for ceramic, Mater. Chem. Phys. (2022) 280.
- [11] Y. El Jabbar, H. Lakhlifi, R. El Ouatib, L. Er-Rakho, S. Guillemet-Fritsch, B. Durand, Preparation and characterisation of green nano-sized ceramic pigments with the spinel structure AB₂O₄ (A = Co, Ni and B = Cr, Al), Solid State Commun. (2021) 334–335.
- [12] M. Llusar, E. García, M.T. García, C. Gargori, J.A. Badenes, G. Monrós, Stability and coloring properties of Ni-qandilite green spinels (Ni,Mg)₂TiO₄: the "half color wheel" of Ni-doped magnesium titanates, Dyes Pigments 122 (2015) 368–381.
- [13] Q. Cheng, X. Chen, L. Liu, P. Jiang, D. Song, M.A. Subramanian, Synthesis and optical properties of Ni/Co/Cr doped BaMg₆Ti₆O₁₉, Ceram. Int. 47 (2021) 34086–34091.
- [14] Y. Wang, Q. Cheng, P. Jiang, L. Liu, K. Cui, Y. Li, Synthesis and properties of novel blue zirconia ceramic based on Co/Ni-doped BaAl₁₂O₁₉ blue chromophore, J. Eur. Ceram. Soc. 42 (2022) 543–551.
- [15] X. Duan, M. Pan, F. Yu, D.J.J.o.A. Yuan, Compounds, Synthesis, Structure and Optical Properties of CoAl₂O₄ Spinel Nanocrystals, vol. 509, 2011, pp. 1079–1083.
- [16] A. Zhang, B. Mu, X. Wang, A.J.A.C.S. Wang, Microwave hydrothermal assisted preparation of CoAl₂O₄/kaolin hybrid pigments for reinforcement coloring and mechanical property of acrylonitrile butadiene styrene 175 (2019) 67–75.
- [17] H. Yang, B. Mu, Q. Wang, J. Xu, A. Wang, Resource and sustainable utilization of quartz sand waste by turning into cobalt blue composite pigments, Ceram. Int. 47 (2021) 13806–13813.
- [18] C. Boucetta, M. Kacimi, A. Ensuque, J.-Y. Piquemal, F. Bozon-Verduraz, M. Ziyad, Oxidative dehydrogenation of propane over chromium-loaded calciumhydroxyapatite, Appl. Catal. Gen. 356 (2009) 201–210.
- [19] Y. Fu, S. Lin, Y. Huang, R. Shi, B. Zhao, Cr⁶⁺ ion doping effects in layered Ca₃Co₄O₉ system, J. Alloys Compd. 613 (2014) 87–92.
- [20] H. Liu, S. Song, A.M. Garbers-Craig, Z.J.C.I. Xue, High-temperature stability of Mg (Al, Cr)₂O₄ spinel co-existing with calcium aluminates in air 45 (2019) 16166–16172
- [21] Q. Cheng, X. Chen, P. Jiang, Q. Wang, Z. Wang, M.A. Subramanian, Synthesis and properties of blue zirconia ceramic based on Ni/Co doped Ba_{0.956}Mg_{0.912}Al_{10.088}O₁₇ blue pigments, J. Eur. Ceram. Soc. 42 (2022) 4311–4319.
- [22] Y. Brik, M. Kacimi, M. Ziyad, F.J.J.o.c. Bozon-Verduraz, Titania-supported cobalt and cobalt-phosphorus catalysts: characterization and performances in ethane oxidative dehydrogenation 202 (2001) 118–128.
- [23] L. Beaury, J. Derouet, L. Binet, F. Sanz, C. Ruiz-Valero, The blue allotropic form of Co²⁺:Na₂CoP₂O₇: optical and magnetic properties, correlation with crystallographic data, J. Solid State Chem. 177 (2004) 1437–1443.
- [24] I.V. Glazunov, A.M. Malyarevich, K.V. Yumashev, O.S. Dymshits, I.P. Alekseeva, M. Y. Tsenter, K.V. Bogdanov, S.S. Zapalova, A.A. Zhilin, Linear and non-linear optical properties of transparent glass-ceramics based on Co²⁺-doped Zn(Al,Ga)₂O₄ spinel nanocrystals, J. Non-Cryst. Solids 557 (2021).
- [25] P. Loiko, O.S. Dymshits, V.V. Vitkin, N.A. Skoptsov, A.A. Zhilin, D.V. Shemchuk, M. Y. Tsenter, K. Bogdanov, A.M. Malyarevich, I.V. Glazunov, X. Mateos, K. V. Yumashev, Saturable absorber: transparent glass-ceramics based on a mixture of Co:beta-Zn₂SiO₄ and Co:ZnO nanocrystals, Appl. Opt. 55 (2016) 5505–5512.
- [26] M. Llusar, A. Zielinska, M.A. Tena, J.A. Badenes, G. Monrós, Blue-violet ceramic pigments based on Co and Mg Co_{2-x}Mg_xP₂O₇ diphosphates, J. Eur. Ceram. Soc. 30 (2010) 1887–1896.
- [27] A.K.V. Raj, P.P. Rao, Intense blue chromophores in cobalt doped phenacite-type zinc germanate system through jahn-teller distortion of Co tetrahedron, ChemistrySelect 6 (2021) 11344–11351.
- [28] L. Desouza, J. Zamian, G. Darochafilho, L. Soledade, I. Dossantos, A. Souza, T. Scheller, R. Angelica, C. Dacosta, Blue pigments based on Co_xZn_{1-x}Al₂O₄ spinels synthesized by the polymeric precursor method, Dyes Pigments 81 (2009) 187–192
- [29] D.K. Sardar, J.B. Gruber, B. Zandi, M. Ferry, M.R. Kokta, Spectroscopic properties of Co²⁺ in related spinels, J. Appl. Phys. 91 (2002) 4846–4852.
- [30] R.S. Pavlov, V.B. Marzá, J.B. Carda, Electronic absorption spectroscopy and colour of chromium-doped solids, J. Mater. Chem. 12 (2002) 2825–2832.

- [31] B. Tian, C. Li, J.J.C.e.j. Zhang, One-step preparation, characterization and visible-light photocatalytic activity of Cr-doped ${\rm TiO_2}$ with anatase and rutile bicrystalline phases 191 (2012) 402–409.
- [32] S.R. Prim, A. García, R. Galindo, S. Cerro, M. Llusar, M.V. Folgueras, G. Monrós, Pink ceramic pigments based on chromium doped M(Al_{2-x}Cr_x)O₄, M=Mg, Zn, normal spinel, Ceram. Int. 39 (2013) 6981–6989.
- [33] Q. Yong, D. Xu, Q. Liu, Y. Xiao, D. Wei, Advances in polymer-based matte coatings: a review, Polym. Adv. Technol. 33 (2021) 5–19.